Isotropic–Liquid Crystal Phase Equilibrium in Semiflexible Polymer Solutions: Effects of Molecular Weight and Ionic Strength in Polyelectrolyte Solutions

Shin-ichiro Inatomi, Yuji Jinbo, Takahiro Sato,* and Akio Teramoto

Department of Macromolecular Science, Osaka University, Toyonaka, Osaka 560, Japan

Received March 16, 1992; Revised Manuscript Received June 8, 1992

ABSTRACT: The isotropic–liquid crystal (cholesteric) phase boundary concentrations for aqueous solutions of xanthan, an ionic double-helical polysaccharide, were determined as functions of the molecular weight of xanthan and the added sodium chloride concentration. The phase boundary concentrations increased sharply with decreasing molecular weight at low molecular weights, as in the case of neutral stiff polymer solutions, and depended strongly on the added salt concentration. The latter dependence demonstrates the importance of the electrostatic interaction between polymers in the isotropic–liquid crystal phase equilibrium. These experimental results were compared with two theories: the Onsager theory extended by Odijk to semiflexible polyelectrolyte solutions and a perturbation theory proposed by us (Sato, T.; Teramoto, A. *Physica A* **1991**, *176*, 72). The latter theory succeeded in almost quantitative prediction of the experimental phase boundary concentrations for xanthan. The same comparison was performed on two other rigid polyion systems: tobacco mosaic virus and DNA.

Introduction

It is well known that solutions of both rodlike and semiflexible polymers can form liquid crystal (nematic or cholesteric) phases above certain critical concentrations. These liquid crystalline polymers can be divided into two categories: neutral and charged stiff polymers. The former category includes, e.g., α-helical polypeptides, schizophyllan, cellulose derivatives, and polyisocyanates, while the latter category contains rodlike viruses, DNA, xanthan, and so on.

For neutral stiff-chain polymer solutions, both experimental and theoretical work has been made extensively on the isotropic–liquid crystal phase behavior and theories of the Onsager type[1-6] have been successful in predicting the experimental isotropic–liquid crystal phase boundaries of many lyotropic polymer systems. Recent papers[5-8] and a review[3] demonstrate this achievement. On the other hand, experimental work on stiff polyelectrolyte systems has not been accumulated, and hence the validity of the Onsager-type theories[1,3,9] considering the long-range electrostatic interaction between polyions has not been critically examined as yet.

Among possible candidates for liquid crystalline polyelectrolytes, we have chosen xanthan, an ionic double-helical polysaccharide, which has been well characterized from dilute solution studies;[10-13] its conformation is represented by a wormlike chain with the persistence length as large as 120 nm[12] and almost independent of salt concentration above 0.01 M.[13] In a recent study,[14] the isotropic–cholesteric phase boundary concentrations were determined as a function of salt concentration for one xanthan sample with the axial ratio of 144. The results were compared with the Onsager theory[1] extended by Odijk[3] to the semiflexible polyelectrolyte solution[14] and with a perturbation theory developed by us.[9] The latter theory, which takes the hard-core potential of the polymer as the reference potential and the electrostatic potential as a thermodynamic perturbation, considers all virial terms for the reference state but only the first-order perturbation (or the electrostatic second virial) term. The perturbation theory was shown to predict almost quantitatively the experimental phase boundary concentrations of the xanthan sample with no adjustable parameters.[9]

However, the same theory could not predict successfully the isotropic–liquid crystal coexisting phase concentrations of aqueous solutions of tobacco mosaic virus with the axial ratio of 16.7 reported recently by Fraden et al.[15] This contradiction might be ascribed to different contributions of the neglected higher-order perturbation terms to the phase boundaries of the two polymer systems,[9] because tobacco mosaic virus has the much smaller axial ratio and then the higher phase boundary concentrations than the xanthan sample examined in the previous study.

In order to make this point clear, we have studied the molecular weight dependence of the phase boundary concentrations for aqueous xanthan. For neutral stiff polymer solutions, it is well known that the polymer molecular weight (or the axial ratio) is an essential parameter to the isotropic–liquid crystal phase boundary.[7,16-19] However, to the best of our knowledge, the molecular weight dependence of the phase behavior in stiff polyelectrolyte solutions has not been investigated so far.

This paper presents the isotropic–liquid crystal phase boundary concentration data for six well-fractionated samples of xanthan with different molecular weights at three different added sodium chloride (NaCl) concentrations (0.01, 0.1, and 1.0 M) and compares them with the previous perturbation theory, along with the Onsager theory extended to wormlike polyelectrolyte solutions. It is necessary to use narrow distribution samples for unambiguous comparison with the theories, and xanthan is suitable for this purpose, because previous dilute solution studies[10-12] established a method for obtaining fairly sharp distribution samples.

Experimental Section

A commercial xanthan sample, Kelco's Keltrol, was sonicated in 1 wt % aqueous solution using 10-kHz sonic irradiation (Cho-Onpa Kogyo Model USV-150N10; 150 kW) for 10, 20, or 72 h. The sonicated samples were purified by centrifugation, fractionated repeatedly, and converted to the sodium salt form following the procedure established before.[10] Each of five selected samples was further divided into three parts by isotropic–liquid crystal phase separations,[20] and every middle fraction was used in the following phase equilibrium experiment. A stock sample named X9-3-3 was added to the phase equilibrium experiment. This sample had also been fractionated by repeating fractional precipitation and the liquid crystal phase separation.

0024-9297/92/2225-5013$03.00/0

Table I
Molecular Characteristics of the Xanthan Samples Used

sample	$[\eta]^a/(10^2\ cm^3\ g^{-1})$	$M_v{}^b/10^4$	N	M_z/M_w
S6-5	0.588	11.0	0.236	
S6-4	0.844	14.2	0.305	
		15.0[c]		1.09
S4-5	1.67	22.8	0.490	
		23.6[c]		1.05
S2-3	3.34	37.8	0.812	
S4-2	4.32	46.0	0.988	
K-7[d]	6.04	61.4	1.32	
X9-3-3	11.03	98.0	2.10	

[a] The intrinsic viscosity in 0.1 M aqueous NaCl at 25 °C. [b] Estimated from the intrinsic viscosity–molecular weight relation obtained by Sato et al.[12] [c] The weight-average molecular weight determined by the sedimentation equilibrium method. [d] The sample used in the previous study.[14]

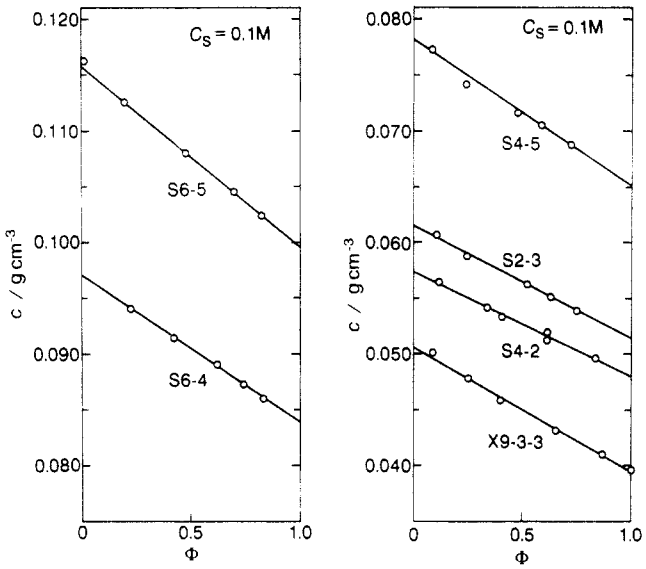

Figure 1. Average concentration c vs the volume Φ of the isotropic phase relative to the whole solution for six xanthan samples in aqueous NaCl with C_s = 0.1 M at 25 °C.

Table I lists the viscosity-average molecular weight M_v and the number N of the Kuhn statistical segments calculated from M_v for each sample, together with the molecular weight per unit contour length M_L = 1940 nm^{-1} and the persistence length q = 120 nm.[12] Sedimentation equilibrium measurements were made for two samples, S6-4 and S4-5 (cf. ref 10 for detailed procedure). Table I also contains the results of the sedimentation equilibrium experiment. The weight-average molecular weight M_w for each sample agrees with M_v within an experimental error. The ratios of the z-average molecular weight M_z to M_w are less than 1.1 for both samples, and all the samples are regarded as monodisperse in the analysis to follow.

The isotropic–liquid crystal phase equilibrium experiment was made by the procedure employed before[7,14] to obtain the relation between the average concentration of biphasic solution and the volume of the isotropic phase relative to the whole solution. The phase boundary concentration was determined from this relation (see below). The temperature was fixed at 25 °C.

Results

Figure 1 illustrates the results of the phase equilibrium experiment for six samples of xanthan dissolved in aqueous NaCl with a NaCl molar concentration C_s = 0.1 M. Here c is the average mass concentration of the biphasic solution and Φ is the volume fraction of the isotropic phase in the whole solution. The data points for each sample almost follow a straight line. Similar linear plots were obtained also for C_s = 0.01 and 1.0 M. These results mean that the presence of the third component, NaCl, in the xanthan solutions does not infringe the linear relation between c and Φ; i.e., the present ternary systems investigated behave nearly as *binary systems* with respect to this linear relation.

Table II
Numerical Results for the Isotropic–Cholesteric Phase Boundary Concentrations c_i and c_a of Solutions of Xanthan in Aqueous Sodium Chloride at 25 °C

sample	c_i/(g cm^{-3})	c_a/(g cm^{-3})	c_a/c_i
	C_s = 0.01 M		
S6-5	0.0659	0.0781	1.19
S6-4	0.0485	0.0577	1.19
S4-5	0.0316	0.0382	1.21
S2-3	0.0218	0.0267	1.22
S4-2	0.0198	0.0249	1.26
K-7[a]	0.0194	0.0168	1.21
X9-3-3	0.0152	0.0192	1.26
	C_s = 0.1 M		
S6-5	0.0996	0.116	1.16
S6-4	0.0839	0.0971	1.16
S4-5	0.0651	0.0782	1.20
S2-3	0.0514	0.0615	1.20
S4-2	0.0480	0.0574	1.20
K-7[a]	0.0454	0.0541	1.19
X9-3-3	0.0394	0.0506	1.28
	C_s = 1.0 M		
S6-5	0.144	0.172	1.20
S6-4	0.125	0.147	1.18
S4-5	0.102	0.121	1.19
S2-3	0.0822	0.0974	1.19
S4-2	0.0778	0.0920	1.18
K-7[a]	0.0760	0.0900	1.18
X9-3-3	0.066 ● 0.001[b]		

[a] The results obtained in the previous study.[14] [b] The value determined by polarizing microscopy.

The two phase boundary mass concentrations c_a (between the biphasic and liquid crystal phase regions) and c_i (between the biphasic and the isotropic phase regions) can be obtained from the linear extrapolation of the c–Φ plots to Φ = 0 and 1, respectively. However, for the highest molecular weight sample X9-3 at C_s = 1.0 M, the viscosity of the biphasic solution was too high to achieve a complete phase separation. Therefore, for this solution, polarizing microscopy was used to find the concentration where the optical anisotropy just disappeared, and this concentration was taken as c_i; the other phase boundary concentration c_a was not determined for this solution. The numerical results obtained are summarized in Table II.

Figure 2 shows the molecular weight dependence of the phase boundary concentrations c_i and c_a determined from the phase equilibrium experiments for aqueous xanthan with C_s = 0.01, 0.1, and 1.0 M at 25 °C. (This figure also includes the data points for $M_v = 6.14 \times 10^5$ which were obtained in the previous study.[14]) With increasing molecular weight, both phase boundary concentrations for every C_s decrease sharply at $M_v \lesssim 4 \times 10^5$ and tend to approach some asymptotic values above that molecular weight. This molecular weight almost corresponds to one Kuhn statistical segment. This molecular weight dependence for aqueous xanthan resembles qualitatively those for solutions of neutral stiff polymers, e.g., poly(γ-benzyl L-glutamate),[16] schizophyllan,[19] poly(hexyl isocyanate),[7,17] and (hydroxypropyl)cellulose.[18]

The phase boundary concentrations shown in Figure 2 exhibit a strong added salt concentration (or ionic strength) dependence in the whole molecular weight range examined. This strong C_s dependence demonstrates an important role of the electrostatic interaction between polyions in the isotropic–liquid crystal phase equilibrium. A similar demonstration was recently made by Fraden et al.[15] who studied the isotropic–liquid crystal phase behavior of the

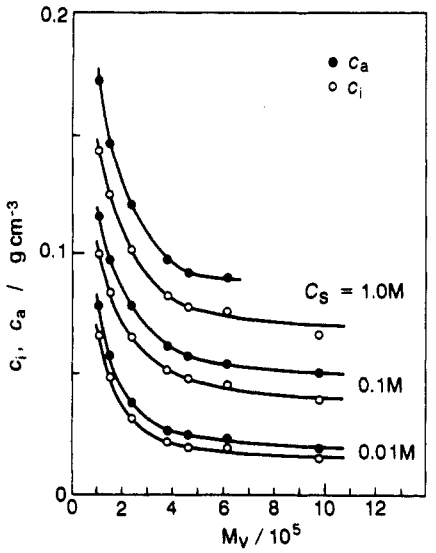

Figure 2. Molecular weight dependence of the phase boundary concentrations c_i between the isotropic phase and biphasic regions and c_a between the anisotropic and biphasic regions for xanthan in aqueous NaCl with C_s = 0.01, 0.1, and 1.0 M at 25 °C.

aqueous solution of tobacco mosaic virus, a charged rodlike virus.

Discussion

Comparison with Theories. (1) Extended Onsager Theory. In a previous paper,[14] the phase boundary concentrations c_i and c_a for aqueous solutions of a xanthan sample with $M_v = 6.14 \times 10^5$ were compared with the Onsager theory[1] extended by Odijk[3] to semiflexible polyelectrolyte solutions. In the first part of this section, we compare the molecular weight dependences of c_i and c_a for aqueous xanthan with this extended Onsager theory, after briefly reviewing the theory.

This theory uses a charged wormlike cylinder model which has the axial contour length L, the number of the Kuhn statistical segments N, the hard-core diameter d, and the linear charge density ν. Its intermolecular potential is expressed as the sum of the hard-core potential u_0 and the electrostatic one w. These potentials are represented by

$$u_0 = \begin{cases} \infty \text{ (when the hard cores of two polymers overlap)} \\ 0 \text{ (otherwise)} \end{cases} \quad (1)$$

and

$$w = \begin{cases} 0 \text{ (when the hard cores of two polymers overlap)} \\ w_2(1,2) \text{ (otherwise)} \end{cases} \quad (2)$$

In general, $w_2(1,2)$ is a function of the relative position and conformations of two interacting wormlike polyelectrolytes 1 and 2. It should be noted that the contributions of u_0 and w to the binary cluster integral are additive, because they do not overlap in the configurational space.

The isotropic–nematic phase boundary concentrations for a solution of such charged wormlike cylinders can be calculated from the excess free energy ΔF of the solution over that of the solvent. When the third and higher virial terms are neglected (the second virial approximation), ΔF is given by[1,3]

$$\Delta F/nk_BT = \mu^\circ/k_BT - 1 + \ln c' - (1/2)(\langle\beta_{1,0}\rangle + \langle\beta_{1,el}\rangle)c' + \sigma \quad (3)$$

where n is the number of polymers in the solution, μ° the standard chemical potential of the solute, and c' the polymer number density. The first three terms on the right-hand side are the chemical potential of an ideal solution. The next two terms represent a nonideality due to the intermolecular excluded volume effect; $\langle\beta_{1,0}\rangle$ and $\langle\beta_{1,el}\rangle$ are the binary cluster integrals with respect to the potentials u_0 and w, respectively, and the angular bracket means the orientational average of two interacting polymers. The final term σ represents an entropy (loss) with respect to the orientational degree of freedom. For rods, σ is the orientational entropy loss of the whole molecule in the nematic phase. On the other hand, for wormlike chains, it is the orientational entropy loss of tangent vectors of each chain at every contour point, and thus includes a conformational entropy loss of the chain in the nematic phase. Khokhlov and Semenov[2] formulated σ for wormlike chains using the Onsager trial function[1] for the orientational distribution function of the chain tangent vectors, although they gave explicit expressions of σ only for N much smaller and much larger than unity. Odijk applied their σ to polyelectrolyte systems.

In a first approximation, flexibility effects on the two cluster integrals $\langle\beta_{1,0}\rangle$ and $\langle\beta_{1,el}\rangle$ were neglected, and the integrals for a charged wormlike cylinder were replaced by those for a charged straight cylinder with the same L, d, and ν.[3] This approximation should be better for stiffer and shorter polymers. In addition, Odijk (and also Onsager) considered only the leading terms in $\langle\beta_{1,0}\rangle$ and $\langle\beta_{1,el}\rangle$ for the corresponding charged straight cylinder which are proportional to L^2 (cf. eqs 4 and 5 in ref 14[21]). This approximation should hold for sufficiently long rigid polyelectrolytes.

The expression of $\langle\beta_{1,el}\rangle$ contains an effective diameter d_{eff}. Onsager calculated d_{eff}, using the Derjaguin approximation[22] for two charged cylinders. On the other hand, Stroobants et al.[23] proposed to calculate d_{eff} from the Philip–Wooding solution[24] of the Poisson–Boltzmann equation for the electrostatic potential of a charged cylinder, and also considered the effect of a twisting force between two charged rods on d_{eff}. Thus, their $\langle\beta_{1,el}\rangle$ contains an orientation-dependent parameter η for the twist effect in addition to the parameter ρ representing the reduction of the polymer excluded volume due to the orientation. In the following, $\langle\beta_{1,el}\rangle$ is calculated from Stroobants et al.'s method, along with using the Debye screening length κ^{-1} at infinite dilution.

Although the above theory is for the isotropic–nematic phase equilibrium, we use this theory for the isotropic–cholesteric phase equilibrium in aqueous xanthan solutions. Since the cholesteric pitch of aqueous xanthan is quite large,[25] the local structure of its cholesteric phase can be regarded as almost identical with that of a nematic phase with the same orientational order parameter. Therefore, the use of eq 3 for the cholesteric phase of aqueous xanthan should be a good approximation.

The phase boundary concentrations c_i and c_a can be calculated from phase coexistence equations with respect to the osmotic pressure and the polymer chemical potential as well as a nematic phase stability equation. These equations are constructed from ΔF of eq 3. This free energy contains three orientation-dependent parameters, ρ, η, and σ. We use for them the expressions of Onsager,[1] Stroobants et al.,[23] and Khokhlov and Semenov,[2] respectively. Since

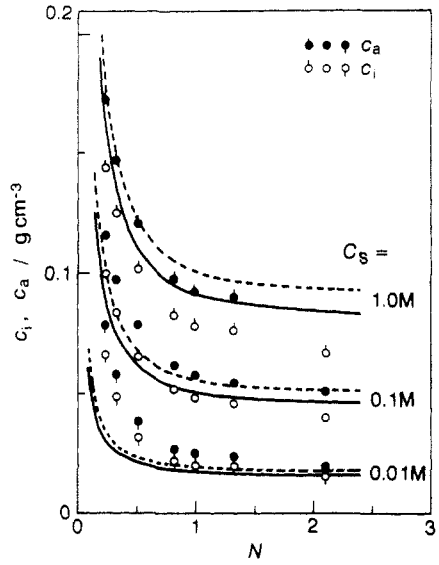

Figure 3. Comparison of the experimental phase boundary concentrations for aqueous xanthan with the Onsager theory[1] extended by Odijk[3] to semiflexible polyelectrolyte solutions: N = the number of Kuhn statistical segments.

the last expression is not valid for N (the Kuhn segment number) ≈ 1, we obtain c_i and c_a at $N \approx 1$ from the interpolation of the c_i and c_a values calculated at $N \geq 1.5$ and $N = 0$ as before.[5,14]

Figure 3 compares the phase boundary concentrations c_i and c_a calculated from the above extended Onsager theory (curves) with the experimental data for aqueous xanthan (circles). The calculation was made for the following four molecular parameters of the polymer: the hard core diameter $d = 2.2$ nm, the linear charge density $\nu = 3.0$ (elementary charge)/nm, the molecular weight per unit contour length $M_L = 1940$ nm^{-1}, and the persistence length $q = 120$ nm, all of which had been determined in the previous dilute solution study on xanthan.[12,13] (The last parameter q was demonstrated to be independent of C_s within experimental error in q at $C_s \geq 0.01$ M.[13]) The values of L and N for each sample were estimated from the molecular weight along with the above M_L and q. Therefore, the theoretical curves in Figure 3 contain no adjustable parameters. The agreement between the theory and experiment is almost quantitative at $C_s = 0.1$ M. On the other hand, the theory underestimates c_i and c_a of lower molecular weight samples at lower ionic strength ($C_s = 0.01$ M), while it overestimates c_i and c_a in the whole molecular weight range at higher ionic strength ($C_s = 1.0$ M). Similar disagreement between the extended Onsager theory and experiment in the phase boundary concentrations has already been observed for one xanthan sample in the previous study.[14]

(2) Perturbation Theory. Recently we[9] presented a perturbation theory to calculate the phase boundary concentrations c_i and c_a for stiff polyelectrolyte solutions. The model used in this theory is charged wormlike spherocylinders interacting with each other by the two potentials u_0 and w which are given by eqs 1 and 2, respectively. We take the hard-spherocylinder system with $w = 0$ as a reference system and considered the electrostatic potential w as a thermodynamic perturbation. This theory improves the above extended Onsager theory with respect to the following three points: this theory takes into account (1) the third and higher virial terms with respect to the hard-core (reference) potential, (2) finite length effects of polyions on the electrostatic interaction between two polyions and $\beta_{1,el}$,[26] and (3) the contribution of polyelectrolyte to the ionic strength in solution.

Instead of eq 3, ΔF used in the perturbation theory is given by

$$\Delta F/nk_BT = \mu^\circ/k_BT - 1 + \ln c' + \sigma + \langle B_0\rangle - (1/2)\langle\beta_{1,el}\rangle c' \quad (4)$$

where $\langle B_0\rangle$ represents all the virial expansion terms of the hard-spherocylinder (reference) system which are averaged over the orientations of all interacting polymers and $\langle\beta_{1,el}\rangle$ corresponds to the first-order perturbation term. We neglect the higher perturbation terms; this approximation corresponds to the second virial approximation for the electrostatic potential w.

The expression of $\langle B_0\rangle$ is given by the scaled particle theory of Cotter[27] for hard-spherocylinder systems (cf. eq 16 in ref 9), while $\langle\beta_{1,el}\rangle$ can be calculated from the effective length L_{eff} and effective diameter d_{eff} (cf. eq 30 together with eqs 28, 29, and 31–34 of ref 9). Here L_{eff} has been introduced in order to take into account a finite length effect of polyions on the electrostatic interaction between two polyions. As in the extended Onsager theory, this theory also neglects flexibility effects on $\langle B_0\rangle$ and $\langle\beta_{1,el}\rangle$.

We proposed to calculate $\langle\beta_{1,el}\rangle$ using an *effective* Debye screening length κ^{-1} in nondilute polyelectrolyte solutions along with the Philip–Wooding solution[24] of the Poisson–Boltzmann equation for a charged cylinder. When all the mobile ions are monovalent, the screening lengths κ_i^{-1} in the isotropic phase and κ_a^{-1} in the anisotropic phase may be given by[9,14]

$$\kappa_\sigma^2 = 8\pi Q[n_{s\sigma}(\Phi) + \Gamma z_p c'_\sigma(\Phi)] \qquad \sigma = i, a \quad (5)$$

Here Q is the Bjerrum length, Γ the Donnan salt exclusion coefficient, z_p the valence of the polyion, and $n_{s\sigma}(\Phi)$ and $c'_\sigma(\Phi)$ the number concentrations of the added salt and polymer, respectively. (The subscripts σ = i and a stand for the isotropic and anisotropic phases, respectively.) The second term on the right-hand side takes into account the contribution of the polyelectrolyte to the electrostatic screening effect. Both the concentrations $n_{s\sigma}(\Phi)$ and $c'_\sigma(\Phi)$ are functions of the volume fraction Φ of the isotropic phase in the whole solution, because the redistribution of the small mobile ions between the coexisting two phases depends on Φ.[9,14]

In this paper, we calculate the phase boundary concentrations using the expressions of the orientation-dependent parameters ρ, η, and σ slightly different from those used in a previous paper.[9] The parameters ρ and η are given in the forms of the asymptotic expansion of α which is the orientational parameter appearing in the Onsager trial function for the orientational distribution function:[1,23]

$$\rho(\alpha) = \frac{4}{(\pi\alpha)^{1/2}}(1 + 2e^{-2\alpha}) \times \left[1 - \frac{30}{32\alpha} + \frac{210}{(32\alpha)^2} + \frac{1260}{(32\alpha)^3} + \frac{20790}{(32\alpha)^4}\right] \quad (6)$$

and

$$\eta(\alpha) = (1/2)(\ln\alpha - 1 - 2\ln 2 + \gamma_E)\rho(\alpha) + \frac{1}{(\pi\alpha)^{1/2}\alpha}\left[5 - \frac{134}{32\alpha} - \frac{614}{(32\alpha)^2} - \frac{1.1}{(32\alpha)^3}\right] \quad (7)$$

(γ_E = the Euler constant). Here we have added the term of α^{-4} to each asymptotic expansion, which was neglected in the previous work. This term may be important for low molecular weight samples at low ionic strength, where α in the coexisting liquid crystal phase becomes considerably small.

Khokhlov and Semenov[2] calculated the entropy loss parameter σ for wormlike chains at the nematic transformation using the Onsager trial function[1] for the orientational distribution function of the tangent vectors to the wormlike chain contour. However, their calculation was limited to the two cases that the number of the Kuhn statistical segments N is much smaller than unity (near the rod limit) and much larger than unity. (In a previous paper,[9] we obtained the phase boundary concentrations c_i and c_a from the interpolation of the c_i and c_a values calculated at $N \geq 1.5$ and $N = 0$.) Later Odijk[3] calculated σ for wormlike chains by a path integral method using a Gaussian distribution function instead of the Onsager trial function. Although his σ is applicable for any value of N, his Gaussian distribution function is, unfortunately, less accurate than Onsager's and his σ does not agree with the Khokhlov–Semenov σ at $N \approx 0$ and $N \gg 1$. Recently DuPré and Yang[8] modified Odijk's σ empirically and obtained an expression of σ which is applicable for any value of N and agrees with that of Khokhlov–Semenov at $N \ll 1$ and $N \gg 1$.[28] Their σ is written as

$$\sigma = \ln \alpha - 1 + \pi e^{-\alpha} + (1/3)N(\alpha - 1) + (5/12) \ln \{\cosh [(2/5)N(\alpha - 1)]\} \quad (8)$$

In this paper, we use this expression for σ.

There are five unknown parameters $c_i'(\Phi)$, $c_a'(\Phi)$, $n_{si}(\Phi)$, $n_{sa}(\Phi)$, and α in the present theory. Among them, $n_{si}(\Phi)$ and $n_{sa}(\Phi)$ are related to each other by the mass conservation rule:

$$n_{si}(\Phi)\Phi + n_{sa}(\Phi)(1 - \Phi) = C_s/N_A \quad (9)$$

where C_s is the average molar concentration of the added salt and N_A is Avogadro's number. In addition to this rule, we have the stability condition of the nematic phase

$$\partial \Delta F_a/\partial \alpha = 0 \quad (10)$$

and three phase coexistence equations with respect to the osmotic pressure Π, the chemical potential of the polyelectrolyte μ, and the activity of small mobile ions:

$$\Pi_i = \Pi_a \quad (11)$$

$$\mu_i = \mu_a \quad (12)$$

$$\gamma_{\pm i} n_{si}(\Phi)[n_{si}(\Phi) + z_p c_i'(\Phi)] = \gamma_{\pm s} n_{sa}(\Phi) \times [n_{sa}(\Phi) + z_p c_a'(\Phi)] \quad (13)$$

Here the subscripts i and a represent the isotropic and anisotropic (nematic) phases, respectively, and $\gamma_\pm$ is the mean activity coefficient of the mobile ions. The expressions of Π and μ are derived from the free energy ΔF in eq 4 (cf. eqs 36 and 37 of ref 9), while that of $\gamma_\pm$ is given from Manning's theory[29] for polyelectrolyte solutions (cf. eq A4 of ref 14; in this equation, ξ is the Manning charge density parameter[29] and $X = \xi^{-1} z_p c'/n_s$).

When C_s and Φ are given, the five unknown parameters can be calculated numerically from the five eqs 9–13. It should be noted that the Debye length κ^{-1} in each phase included in eqs 10–12 must be calculated from eq 5; the Donnan salt exclusion coefficient Γ in this equation can be calculated from the equation $\Gamma = 1/(4\xi)$.[29] The experimental phase boundary mass concentrations c_i and c_a correspond to $c_i'(1)(M/N_A)$ and $c_a'(0)(M/N_A)$, respectively, calculated from the present perturbation theory along with the molecular weight M of the polymer.

In Figure 4, the values of c_i and c_a calculated from the above perturbation theory are compared with the experimental results for aqueous xanthan. The molecular parameters of the xanthan double helix used in the calculation are the same as in the previous section, and then no adjustable parameter is used for the calculation. Comparing this figure with Figure 3, it can be seen that the agreement between theory and experiment is improved in Figure 4 at $C_s = 0.01$ and 1.0 M, although an appreciable disagreement at $C_s = 0.01$ M is still observed in the lower molecular weight range. (At $C_s = 0.1$ M, the curves of c_i and c_a for the perturbation theory are almost identical with those for the extended Onsager theory.[3]) The improvement at $C_s = 1.0$ M is due to the higher virial terms for the hard-core interaction, because c_i and c_a become high at high C_s. On the other hand, the improvement at $C_s = 0.01$ M is ascribed both to the contribution of the polyelectrolyte to κ_i and κ_a and to the reduction of the effective (cylinder) length L_{eff} of the polyion by the polyion-end effect on the electrostatic interaction. The imperfectness of the fitting at low C_s and low molecular weight is suggested to arise mainly from approximations used to take these two effects into account; the higher order perturbation (electrostatic) terms neglected in the theory should be a factor to reduce the theoretical phase boundary concentrations.

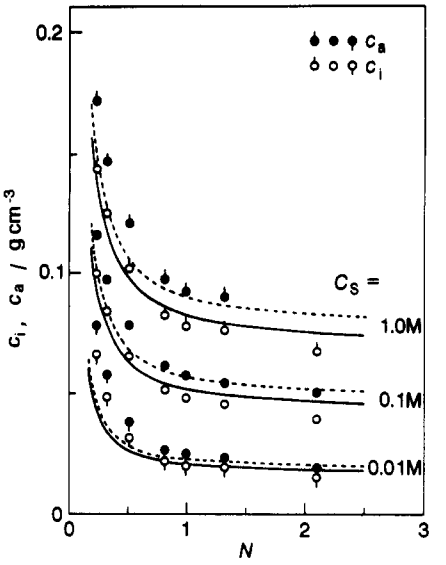

Figure 4. Comparison of the experimental phase boundary concentrations for aqueous xanthan with the perturbation theory (see text).

In order to examine the relation between the average mass concentration c and the volume fraction Φ of the isotropic phase for biphasic solutions of xanthan, we have calculated $c_i'(\Phi)$ and $c_a'(\Phi)$ as functions of Φ at fixed C_s. Figure 5 shows the results of the coexisting phase mass concentrations $c_i(\Phi)$ ($\equiv c_i'(\Phi)M/N_A$) and $c_a(\Phi)$ ($\equiv c_a'(\Phi)M/N_A$) calculated for xanthan with the molecular weight of 38×10^4 ($N = 0.812$) at $C_s = 0.1$ M. Both $c_i(\Phi)$ and $c_a(\Phi)$ are slightly decreasing functions of Φ. The average mass concentration c in biphasic solutions is calculated from $c_i(\Phi)$ and $c_a(\Phi)$ using the relation

$$c = c_i(\Phi)\Phi + c_a(\Phi)(1 - \Phi) \quad (14)$$

As shown by the filled circles in Figure 5, the plot of c vs Φ obtained from the calculated coexisting phase concentrations is linear in a very good approximation. This theoretical result justifies the procedure for obtaining c_i and c_a from the linear extrapolation of the c vs Φ relation, as exemplified in Figure 1. Similar calculations for different C_s and molecular parameters also gave linear relations between c and Φ. Therefore, we can say that the ternary system of polyelectrolyte and aqueous salt behaves like a binary system with respect to the c vs Φ relation.

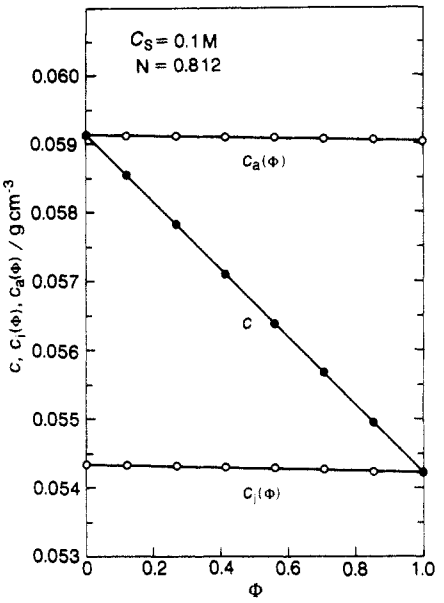

Figure 5. Coexisting isotropic and anisotropic phase mass concentrations $c_i(\Phi)$ and $c_a(\Phi)$ and the average mass concentration c calculated from the perturbation theory for biphasic solutions of xanthan with the molecular weight 38×10^4 ($N = 0.812$) at $C_s = 0.1$ M. Φ = the volume fraction of the isotropic phase in the whole solution.

Comparison of the Perturbation Theory with Other Experiments. As shown in a previous paper (cf. solid curves in Figure 4 of ref 9), the above perturbation theory overestimated the isotropic–liquid crystal coexisting phase concentrations for the tobacco mosaic virus solution obtained by Fraden et al.[15] over the whole range of added salt concentration examined (0.0018 M < C_s < 0.06 M). As mentioned above, the previous work used different expressions of the three orientation-dependent parameters σ, ρ, and η. However, since eq 3 for σ approaches the Onsager σ^1 used in the previous paper at the rod limit (tobacco mosaic virus can be regarded as a rigid rod) and the orientation parameter α of the coexisting liquid crystal phase is considerably large for tobacco mosaic virus, the results of the phase boundary concentrations have not been affected by using slightly modified expressions of the parameters.

The tobacco mosaic virus is known to have the length of 300 nm and the diameter of 18 nm, and then the axial ratio of 16.7.[30] This axial ratio is not much different from that of the lowest molecular weight sample of xanthan used in this study (~26).[31] This implies that the contribution of the higher (electrostatic) perturbation terms to c_i and c_a for tobacco mosaic virus is comparable to that for lower molecular weight xanthan. Although the electrostatic ternary and higher cluster integrals have not been formulated yet, it seems impossible that the higher electrostatic perturbation terms would improve the perturbation theory to agree with data of both tobacco mosaic virus and xanthan systems, because the theoretical phase boundary concentrations deviate from the experimental data in the opposite directions for tobacco mosaic virus and low molecular weight xanthan at low C_s. For the same reason, improvement of the theory is hardly accomplished for both systems by reconsiderations of the polyion-end effects on $\langle\beta_{1,el}\rangle$ nor of the polyion contribution to the electrostatic screening effect.[32] We cannot explain the disagreement between the theory and experiment for tobacco mosaic virus at present.

Recently Rill[33] and Strzelecka and Rill[34-36] measured the isotropic–cholesteric phase boundary concentrations for aqueous solutions of DNA, another stiff polyelectrolyte. All the phase equilibrium experiments were made by using the DNA sample of 146 base pairs which has the contour length of 48.5 nm. It is known that the DNA molecule has the hard-core diameter of 2.5 nm, the linear charge density of 6.1 (elementary charge)/nm,[37] and the persistence length of about 50 nm.[3] Therefore, DNA is a more highly charged and more flexible polyelectrolyte than xanthan; the axial ratio of the DNA sample used in refs 33–36 is 19.4 and almost the same as our lowest molecular weight sample of xanthan.

Table III
Comparison of Experimental Phase Boundary Concentrations for Aqueous DNA with the Perturbation Theory

		experiment			perturbation theory	
C_s/M	T/°C	c_i/(g cm^{-3})	c_a/(g cm^{-3})	c_a/c_i	c_i/(g cm^{-3})	c_a/(g cm^{-3})
2	30	0.180[a]	0.210[a]	1.2	0.169	0.180
0.21	20	0.123[b]	0.152[b]	1.24	0.139	0.148
1.0	20	0.170[c]	0.272[c]	1.6	0.163	0.174
0.1	20	0.136[c]	0.271[c]	2.0	0.122	0.130
0.01	20	0.131[c]	0.255[c]	1.95	0.068	0.072

[a] Reference 33. [b] Reference 34. [c] Reference 36.

Table III compares their experimental results with the perturbation theory.[38] The perturbation theory can predict experimental data of c_i and c_a at $C_s = 0.21$ M and of c_i at $C_s = 2$ M almost quantitatively, while it slightly underestimates c_a at $C_s = 2$ M. Much larger disagreement is seen for the most recent data of c_a at $C_s = 0.01$, 0.1, and 1.0 M, as well as c_i at $C_s = 0.01$ M.[39] It should be noticed, however, that the new data[35,36] show a much wider phase gap or larger ratio c_a/c_i than the previous data, and further the researchers reported a new phase called "the precholesteric phase" appearing between c_i and c_a, which had not been observed in the previous studies.[33,34] The researchers did not mention the reason for these *qualitative* differences between the new and previous data. Our phase boundary data of aqueous xanthan seem to be more compatible with the older data of aqueous DNA than with the new data.

Strzelecka and Rill[35,36] showed plots for aqueous DNA determined by ^{31}P NMR similar to Figure 1 in the present paper (cf. Figure 5 of ref 35 and Figure 2 of ref 36); their C and Cf_a are the average mass concentration c of the polymer and the quantity equivalent to $c_a(1 - \Phi)$ in the present paper, respectively. Their plots of $c_a(1 - \Phi)$ vs c were nonlinear unlike our plots of c vs Φ in Figure 1. Previously nonlinear plots of c vs Φ were obtained for a xanthan sample which was not fractionated by the isotropic–liquid crystal phase separation.[40] By replotting these data in the way of $c_a(1 - \Phi)$ vs c, the data points followed a convex curve similar to Strzelecka and Rill's data at lower temperature. Moreover, the extrapolation to $\Phi = 0$ of the nonlinear plots of c vs Φ gave much higher apparent c_a than those obtained after the fractionation by the isotropic–liquid crystal phase separation. This nonlinearity was attributed to a tiny amount of denatured xanthan without the helical conformation. Such xanthan may not form the liquid crystal phase but remain in the isotropic phase, so that apparent c_a should become higher. Similar nonlinearity in the plots of $c_a(1 - \Phi)$ vs c as well as high c_a values obtained by Strzelecka and Rill[35,36] implies the possibility of some unfavorable alteration in properties of the DNA sample during the sequential studies. Therefore, it would be premature to seriously take the disagreement between the theory and experiment for DNA shown in Table III.

Acknowledgment. This work was financially supported by a Grant-in-Aid for Scientific Research (No. 01470108) from the Ministry of Education, Science, and Culture of Japan.

References and Notes

(1) Onsager, L. *Ann. N. Y. Acad. Sci.* **1949**, *51*, 627.
(2) Khokhlov, A. R.; Semenov, A. N. *Physica A* **1982**, *112*, 605.
(3) Odijk, T. *Macromolecules* **1986**, *19*, 2313.
(4) Lee, S.-D. *J. Chem. Phys.* **1987**, *87*, 4972.
(5) Sato, T.; Teramoto, A. *Mol. Cryst. Liq. Cryst.* **1990**, *178*, 143.
(6) Hentschke, R. *Macromolecules* **1990**, *23*, 1192.
(7) Itou, T.; Teramoto, A. *Macromolecules* **1988**, *21*, 2225.
(8) DuPré, D. B.; Yang, S. *J. Chem. Phys.* **1991**, *94*, 7466.
(9) Sato, T.; Teramoto, A. *Physica A* **1991**, *176*, 72.
(10) Sato, T.; Norisuye, T.; Fujita, H. *Polym. J.* **1984**, *16*, 341.
(11) Sato, T.; Kojima, S.; Norisuye, T.; Fujita, H. *Polym. J.* **1984**, *16*, 423.
(12) Sato, T.; Norisuye, T.; Fujita, H. *Macromolecules* **1984**, *17*, 2696.
(13) Sho, T.; Sato, T.; Norisuye, T. *Biophys. Chem.* **1986**, *25*, 307.
(14) Sato, T.; Kakihara, T.; Teramoto, A. *Polymer* **1990**, *31*, 824.
(15) Fraden, S.; Maret, G.; Casper, D. L. D.; Meyer, R. B. *Phys. Rev. Lett.* **1989**, *63*, 2068.
(16) Robinson, C.; Ward, J. C.; Beevers, R. B. *Discuss. Faraday Soc.* **1958**, *25*, 29. Itou, T.; Funada, S.; Shibuya, F.; Teramoto, A. *Kobunshi Ronbunshu* **1986**, *43*, 191.
(17) Conio, G.; Bianchi, E.; Ciferri, A.; Krigbaum, W. R. *Macromolecules* **1984**, *17*, 856.
(18) Aden, M. A.; Bianchi, E.; Ciferri, A.; Conio, G.; Tealdi, A. *Macromolecules* **1984**, *17*, 2010.
(19) Itou, T.; Van, K.; Teramoto, A. *J. Appl. Polym. Sci.: Appl. Polym. Symp.* **1985**, *41*, 35.
(20) Itou, T.; Teramoto, A. *Polym. J.* **1984**, *16*, 779.
(21) Equation 5 in ref 14 has an error; the diameter d must be removed from the right-hand side.
(22) Derjaguin, B. *Kolloid-Z.* **1934**, *69*, 155.
(23) Stroobants, A.; Lekkerkerker, H. N. W.; Odijk, T. *Macromolecules* **1986**, *19*, 2232.
(24) Philip, J. R.; Wooding, R. A. *J. Chem. Phys.* **1970**, *52*, 953.
(25) Sato, T.; Kume, H.; Sato, Y.; Teramoto, A. Manuscript in preparation.
(26) A finite length effect of polyions on $\beta_{1,el}$ was considered also by Odijk (Odijk, T. *J. Chem. Phys.* **1990**, *93*, 5172). However, he used a model of *infinitely thin* charged rod, so that his result cannot be applied to the present case as it stands.
(27) Cotter, M. A. *J. Chem. Phys.* **1977**, *66*, 1098. Cotter, M. A. *Phys. Rev. A* **1974**, *10*, 625.
(28) Hentschke[6] also presented an empirical interpolation formula for the Khokhlov–Semenov σ.
(29) Manning, G. S. *J. Chem. Phys.* **1969**, *51*, 924.
(30) Casper, D. L. D. *Adv. Protein Chem.* **1963**, *18*, 37.
(31) An effective axial ratio defined by $L/\langle d_{eff}\rangle_{iso}$ ($\langle d_{eff}\rangle_{iso}$ = the isotropically averaged effective diameter d_{eff}) for the lowest molecular weight xanthan at C_s = 0.01 M is even smaller than that for tobacco mosaic virus at C_s = 0.0018 M.
(32) The charge density of the tobacco mosaic virus has not been determined definitely, but is believed to be 1–2 negative elementary charges per protein subunit, which corresponds to be 7–14 (elementary charge)/nm. However, this ambiguity does not affect the phase boundary concentrations calculated, because the asymptotic electrostatic potential of the charged rod is insensitive to the linear charge density due to the so-called ion condensation effect[29] for such a highly charged polymer.
(33) Rill, R. L. *Proc. Natl. Acad. Sci. U.S.A.* **1986**, *83*, 342.
(34) Strzelecka, T. E.; Rill, R. L. *J. Am. Chem. Soc.* **1987**, *109*, 4513.
(35) Strzelecka, T. E.; Rill, R. L. *Biopolymers* **1990**, *30*, 57.
(36) Strzelecka, T. E.; Rill, R. L. *Macromolecules* **1991**, *24*, 5124.
(37) Nicolai, T.; Mandel, M. *Macromolecules* **1989**, *22*, 438.
(38) Strzelecka and Rill[35,36] compared their phase boundary data with the Onsager theory refined by Stroobants et al.[23] In their calculation of the phase boundary concentrations, they assumed that polyions contributed to the electrostatic screening effect as effective as small ions and used the Debye screening length κ^{-1} calculated from eq 5 with $\Gamma = 1$. However, this overestimates the polyion contribution to the screening effect owing to the ion condensation effect.[29] In addition to this, they did not consider the redistribution of the added salt between the coexisting isotropic and anisotropic phases.[9]
(39) Strzelecka and Rill[36] claimed that the difference in the charge density ν between xanthan and DNA would be responsible for the different conclusions between refs 36 and 14. However, as mentioned in ref 32, the difference in ν is not an important factor due to the ion condensation effect, and we do not agree with their claim. [In ref 36, there is a wrong description of ν of xanthan; it is not 1/30 Å^{-1} but 1/3.3 Å^{-1} (=3 nm^{-1}) and exceeds the critical charge density for the ion condensation (1.4 nm^{-1}).[29]]
(40) Kakihara, T.; Sato, T.; Teramoto, A. Unpublished data.

Registry No. Xanthan, 11138-66-2.